FR8100297

LAPP-EXP-07
JUILLET 1980

PATTERN RECOGNITION IN CALORIMETERS

DELLA-NEGRA M.
L.A.P.P. Annecy le Vieux, FRANCE.

ABSTRACT.

It is probable that LEP detectors will often include 4π calorimeters. Since this is a novel technique, not much expertise exists yet in the field of pattern recognition for large calorimeter systems. A fast method to simulate calorimeter signals, based on an analytical parametrization of electromagnetic and hadronic showers, developped by the UA1 software group on calorimetry, is presented. Some reconstruction problems are discussed, in particular the question of disentangling individual showers within an energetic jet.

1. INTRODUCTION.

Recent developments on jet physics in existing e^+e^- colliders (Spear, Doris, Petra) and speculations on jet physics both in hadron-hadron colliders (ISR, $\bar{p}p$ colliders, ISABELLE) and in future e^+e^- colliders (LEP) have put the emphasis on the need for "4π" calorimetry to detect both electromagnetic and hadronic showers.

Besides jet physics, in a LEP detector "4π" calorimeters are useful for $\gamma\gamma$ physics, μ detection, in which case they act as hadron filters, detection of energetic neutrinos by missing energy, etc...

Since this is a novel technique, not much expertise exists yet in the field of pattern recognition for large calorimeter systems. In particular it is still debatable whether or not one can disentangle closeby showers inside an energetic collimated jet. In any case, to study such a problem and in general to design software reconstruction programs in calorimeters, one has to follow the same strategy as the one usually adopted to tune reconstruction programs in track chamber spectrometers :

(i) Simulation of (calorimeter) signals associated to complex multiparticle events.

(ii) Comparison with test data.

(iii) Try various reconstruction methods.

Such a strategy was followed by the people in charge of the calorimeter software [1] in the UA1 experiment at the CERN SPS proton-antiproton collider [2]. In the central region ($5^\circ < \theta_{cm} < 175^\circ$) the UA1 calorimeter system consists

of fine grained lead-scintillator sandwiches located inside the coil of a "calorimetrized" magnet (iron-scintillator sandwich) [3]. This calorimeter set-up was primarily designed to detect :

(i) The electronic decay of the Z^0, $Z^0 \rightarrow e^+e^-$.

(ii) Large p_t jets in the range

$$20 \text{ GeV/c} \leq p_t \leq 60 \text{ GeV/c}.$$

Hence the physics objectives are very similar to those of a LEP experiment.

It is then probably a useful exercise to describe in some detail, to future LEP physicists, the status and goals of the UA1 calorimeter software. However, one should keep in mind that the work is not final and that all the presented results, in particular those on shower parametrization should be considered as preliminary.

2. SIMULATION OF CALORIMETER SIGNALS.

Monte-Carlo programs exist, which simulate in full detail the development of electromagnetic showers and of hadronic showers [4] ; however, they are not very useful to study "4π" calorimetry problems because :

(i) They are time consuming.

(ii) They are not easy to adapt to a complicated "4π" calorimeter geometry.

Our aim was then to develop a fast method to simulate calorimeter signals based on an analytical parametrization of electromagnetic and hadronic showers.

In a first step one has to follow in the magnetic field each charged ($e^{\pm}$, $\mu^{\pm}$, $\pi^{\pm}$, $K^{\pm}$, p, $\bar{p}$, etc...) and neutral

(γ, n, K^o, etc...) particle produced in a complex event through the various segments of the calorimeter system, in order to compute for the center of each shower how much material, passive (absorbers) or active (scintillators), has been traversed. In order to perform efficiently this geometrical tracking, it is of prime importance to have a computer representation of the calorimeter detector well matched to the chosen tracking algorithm. We found very useful to optimize the decomposition of our calorimeter detector system into various data banks linked together into a calorimeter data structure, in the framework of the Hydra System [5]. Fig.1 shows the finally adopted data structure to represent the full UA1 calorimeter system, including the forward calorimeter arms and the wire planes of position detectors located in some of the forward calorimeters. The whole system is decomposed into 25 Calorimeter Modules, banks CM, corresponding to simple geometrical boxes in space ; to each CM bank is linked a Calorimeter Stack bank, CST describing the longitudinal segmentation of the calorimeter and a CELL bank, CEL, describing the lateral segmentation. From this decomposition follows a logical numbering of the $\sim$ 5000 ADC readings representing the raw signals of the calorimeters which one wants to simulate. Fig.2 shows a computer display of a full event tracked in the central part of the UA1 detector. The lines shown to represent the calorimeter detector indicates the geometrical limits of the calorimeter modules (CM) and limiting surfaces of the longitudinal segments (CST), the limits corresponding

to lateral segmentation (CEL) are not shown. A particle coming from the interaction point sees at normal incidence 4 segments of lead-scintillator sandwiches (24 to 30 radiation lengths depending on the angle of incidence), followed by 2 iron-scintillator segments (return yoke of the magnet, $\sim$ 5 absorption lengths). When departing from normal incidence, the number and the length of the traversed segments may change. This is a general problem for 4π calorimeters.

Intersections with the surfaces defining the longitudinal segments are kept into a track bank.

A fine stepping through each scintillator and absorber plate of a given segment, defined by two successive points of the track bank, is then performed to accumulate L_s the length of scintillator traversed, L_a the length of absorber traversed and to deposit accordingly energy in the scintillator plates and distribute it into the various adjacent cells (lateral segmentation). In order to do that a parametrization of the shower development is necessary. First one needs a parametrization of the mean longitudinal profile of a shower, i.e a distribution of the deposited energy E as a function of depth s :

$$\frac{dE}{ds} = f(s), \qquad (2.1)$$

normalized in such a way that a fully contained shower should deposit all of its incident energy E :

$$\int_0^\infty f(s)ds = E \qquad (2.2)$$

It is well known [6] that, when expressing the depth s in terms of number of radiation lengths s/X_o one can parametrize the longitudinal development of an electromagnetic shower, independently of the absorber composition, with a formula of the type :

$$dE = E \frac{x^{\alpha-1} e^{-x} dx}{\Gamma(x)} \qquad (2.3)$$

where :

.E is the incident energy

.$x = \beta \frac{s}{X_o}$ is the number of radiation lengths multiplied by a dimensionless coefficient β

.α and β are dimensionless coefficients containing the energy dependence of the shape of the shower :

$$\alpha = \alpha_0 + \alpha_1 \log E$$

$$\beta = \beta_0 + \beta_1 \log E$$

The log E dependence is dictated by the observation that the shower maximum and the length of the showers increase like log E. The shower maximum is given by :

$$s_{max} = \frac{(\alpha-1)}{\beta} X_o$$

.$\Gamma(\alpha)$ is the gamma function insuring the normalisation (2.2)

$$\Gamma(\alpha) = \int_0^\infty x^{\alpha-1} e^{-x} dx$$

A good fit to the UA1 data on electromagnetic showers up to E = 92 Gev is obtained with :

$$\alpha = 2.284 + 0.7136 \log E$$

$$\beta = 0.5607 + 0.0093 \log E$$

It was suggested to us by T.Hansl, on the basis of the WA1 data on hadronic showers [7], that after removal of the fluctuation due to the start of the shower s_o, longitudinal profiles of hadronic showers could be parametrized by a two component expression of the form :

$$dE = E\left[c\frac{x^{\alpha_E-1}\,e^{-x}\,dx}{\Gamma(\alpha_E)} + (1-c)\frac{y^{\alpha_H-1}\,e^{-y}\,dy}{\Gamma(\alpha_H)}\right] \qquad (2.4)$$

where :

.E is the incident energy.

.$x = \beta_E \frac{s-s_0}{X_o}$ is the number of radiation lengths accumulated since the start s_0 of the shower multiplied by a dimensionless coefficient β_E .

.$y = \beta_H \frac{s-s_0}{\lambda}$ is the number of absorption lengths accumulated since the start of the shower multiplied by a dimensionless coefficienc β_H (λ is the absorption length).

.c represents the fraction of the electromagnetic component of the hadronic shower.

.α_E, β_E, α_H, β_H are dimensionless coefficients containing the Log E dependence.

.$\Gamma(\alpha_E)$, $\Gamma(\alpha_H)$ are the gamma functions ensuring the normalisation (2.2).

The physical meaning of the two components of expression (2.4) is clear : the first one, which scales like the radiation length, represents the electromagnetic hard core of the shower, the second one, scaling like the absorption length, represents pure hadronic interactions.

Fits of the above expression were tried on various available data on hadronic showers by R.Böck. He soon recognized that data with different ratios X_o/λ were necessary

to differentiate the two components of expression (2.4).

Under his suggestion, data were taken in the UA1 calorimeter test facility on hadronic shower development in a pure lead calorimeter. A simultaneous fit to data in pure iron and pure lead was obtained with the following parameters (fig.3) :

$$c = 0.4634$$

$$\alpha_H = 0.6165 + 0.3183 \log E, \quad \alpha_E = \alpha_H$$

$$\beta_H = 0.9099 - 0.0237 \log E, \quad \beta_E = 0.2198$$

The data on fig.3 are measurements from the shower origin. One can then use expression 2.4, fold it with a distribution of the shower origin of the form $e^{-s/\lambda}$ and integrate it over longitudinal segments. The result is shown on fig.4 and compared to WA1 data from the beginning of the calorimeter and to UA1 data in a mixed calorimeter consisting of 3 lead segments and 4 iron segments. The agreement is good.

Having a reliable model for the mean deposited energy as a function of depth s, one can then proceed to the deposition in the calorimeter cells.

First the energy ΔE_{inc} deposited in a given segment (fig.5b), $s_1 \leq s \leq s_2$, is computed using the parametrization (2.2) or (2.4) (fig.5a), then the energy deposited into the scintillators, ΔE_{scint}, is given by the expression :

$$\Delta E_{scint} = b\Delta E_{inc} \frac{(\frac{dE}{dx})_s L_s}{(\frac{dE}{dx})_s L_s + (\frac{dE}{dx})_a L_a} \qquad (2.5)$$

where :

- b is the fraction of visible energy, of the order of 70 % for hadronic showers and 90 % for electromagnetic showers ; b varies slowly with E_{inc} and the type of absorbers, since it is related to nuclear effects.
- L_s is the length of scintillator seen by the center of the shower for this segment.
- L_a is the corresponding length of absorber.
- $(\frac{dE}{dx})_s$ is the mean energy loss per unit length in the scintillator.
- $(\frac{dE}{dx})_a$ is the mean energy loss per unit length in the absorber.

A discussion of formula (2.5) can be found in [9].

ΔE_{scint} is then distributed laterally into adjacent cells (fig.5c) using for the lateral profile of the shower a 2-dimensional gaussian distribution characterized by a variance σ increasing linearly with the depth s. After attenuation of the light into the scintillator, the ADC signals are then calculated and summed over the showers of the same event going into the same cell. A full simulation of the calorimeter signals is then obtained.

3. COMPARED WITH TEST DATA.

Some comparison with data was already done on fig.3 and 4 in order to justify our parametrization. In the previous section a model was given to simulate the mean deposited energy into calorimeter cells, however in many applications

this is not enough, since hadronic showers encounter very large fluctuations.

It was already necessary to introduce the fluctuation on the start of the shower ; other fluctuations need to be introduced, if one wants to reproduce in detail the energy sharing between longitudinal segments and the correlations between the signals.

A very recent attempt was done by T.P.Shah to simulate fully the fluctuations of a hadronic shower in a prototype iron UAl calorimeter cell consisting of two longitudinal segments, 2.4 absorption length each. More details on the experimental set-up can be found in [8].

He finds that 3 independent fluctuations are sufficient to reproduce the data :

(i) fluctuate the shower origin s_0 according to an exponential law : $e^{-s/\lambda}$.

(ii) fluctuate the incident energy to simulate the energy resolution of the calorimeter, according to a gaussian law

mean : $\mu = E_{inc}$

variance: $\sigma = 0.8 \sqrt{E_{inc}}$

(iii) fluctuate the length of the shower (95 % containment) $L(E_{inc})$, which depends on the incident energy, according to a gaussian law :

mean : $\mu = L(E_{inc})$

variance : $\sigma = 0.45\ L(E_{inc})$

Fig.6 shows for a 10 GeV incident π^- beam a plot of the visible reconstructed energy in the back segment, E_{BACK}, as a function of the visible reconstructed energy in the front segment, E_{FRONT}, large fluctuations are observed together with the expected correlation $E_{FRONT} + E_{BACK} = b\ 10$ GeV, b being the fraction of visible energy already discussed (formula 2.5).

Fig.7 shows the same plot obtained with simulated data, applying the above 3 independent fluctuations.

On fig.8 the simulated data are superimposed to the real data on various projections of the same plot, E_{FRONT}, E_{BACK}, $E_{FRONT} + E_{BACK}$; the agreement is good. A similar agreement is obtained for 60 GeV data. The aim is now to reproduced measurements on mixed calorimetry (lead + iron) at various angles of incidence. Results should be obtained soon.

The next step in the strategy would be now to go in reverse order : start from the simulated calorimeter signals and try to reconstruct full events, i.e, built a reconstruction program.

4. RECONSTRUCTION PROBLEMS IN CALORIMETERS.

Since a complete reconstruction program does not exist yet for the UA1 calorimeters, I cannot base my discussion on quantitative results. I will mention two problems and illustrate them on two concrete extreme examples :

(i) The UA1 end cap electromagnetic calorimeter called "Bouchon" : a lead/scintillator sandwich, complemented by a position detector made of proportionnal tubes of $2 \times 2\ cm^2$ section.

(ii) The liquid argon TASSO electromagnetic calorimeter, finely subdivided into towers and 2 cm wide strips.

The first problem is the reconstruction of individual electromagnetic showers. It is clear that this problem depends strongly on the type of calorimeter ; however all reconstruction techniques rely on the relatively well fixed shape of the electromagnetic shower (small fluctuations).

In particular the transverse size of the electromagnetic shower when expressed in radiation lengths is independent of the absorber and of the energy of the shower and does depend only on the depth expressed in radiation lengths (approximative linear dependence). For example the Bouchon position detector after 11 X_o measures that the transverse profile of an electromagnetic shower is well represented by a gaussian of variance $\sigma = 2$ cm independent of the energy [10].

It is clear that at a given depth where the r.m.s. transverse size of the shower is σ :

(i) The optimum lateral segmentation should be of order σ.

(ii) Close by showers of comparable energies can be disentangle up to a distance $D \geq 2\sigma$.

(iii) The center of gravity of an energetic shower can be reconstructed with a precision of the order of few millimeters.

Fig.9 shows a computer display of a reconstructed electromagnetic shower in a half Bouchon exposed recently to a test electron beam (40 GeV e^-).

Fig.9a and 9b show the reconstructed cluster in the position detector : two planes of orthogonal proportional tubes placed at a depth of 11 X_o. The deposited charge is read on both ends of the wire of each tube, so that each plane measures independently the position of the shower (barycenter of tube coordinate and barycenter of the current division coordinate) and the total deposited charge by the shower at this depth. On fig.9, a tube measurement is represented by a rectangle centered on the position given by current division. The width of the rectangle is 2 cm (tube width), the length of the rectangle is proportional to the total deposited charge in the tube. Fig. 9c shows the correlated measurements in the Bouchon lead/scintillator sandwich divided lateraly into 16 azimuthal sectors or "petals" and longitudinally into 4 segments (3.5 X_o, 7 X_o, 8.4 X_o, 7 X_o). Each segment of each "petal" is seen by a photomultiplier. The position detector shows that petal 11 has been hit ; the 4 longitudinal readings of this petal are indicated on the figure. It is important to notice here that longitudinal segmentation is also a powerful way to recognize the "pattern" of an electromagnetic shower. In particular one can play with the fact that the longitudinal profile of an electromagnetic shower is different from the longitudinal profile of a hadronic shower to achieve a rejection π/e of 10^{-3} in the Bouchon, when combining with momentum measurement in the central detector and asking $p/E = 1$.

Similarly fig.10 shows the pattern of a single electromagnetic shower in the TASSO liquid argon calorimeter [11] at PETRA. It comes from a Bhabba scattering ($e^+e^- \to e^+e^-$) at a c.m.s. energy of 35.5 GeV. Starting from the vertex, the electron deposits its energy into the beam tube and the coil (1.3 X_o), then into front towers 7×7 cm^2 (6 X_o) and finally into back towers, 14×14 cm^2 (8 X_o) so that two longitudinal readings of the shower development are available. The lateral development of the shower, only roughly measured by the towers, is given by 6 planes of orthogonal Z and ϕ strips, 2 cm wide, placed at 3 different depths (1.3 X_o, 2.7 X_o, 4.1 X_o). One can follow on fig.10b, the increase of the lateral width of the shower in the 3 successive planes of Z-strips : 1 strip after 1.3 X_o, 2 strips after 2.7 X_o, 4 strips after 4.1 X_o. Although for this electron most of its energy is contained into one tower ($\sim$ 90 %) the cluster extends into several adjacent towers, showing that it will be difficult to divide the energy into two close by electromagnetic showers.

The question of separating close by showers within an energetic jet is the second problem I want to discuss using the same two calorimeters. Fig.11 shows the deposition of a hadronic jet (E_{jet} = 17.75 GeV) into the liquid argon TASSO calorimeter. In a square of 5×5 front towers, one can see that a certain number of photons deposit their energy together with three charged hadrons ; looking at figure 11b, one sees that even with the help of the ϕ and Z strips it will be extremely difficult, if not impossible,

to disentangle individual showers within the jet. Of course it would be nice to have a hadronic calorimeter in the back, which, in conjunction with the measurements of the central detector, would help to trace back the hadronic showers in the electromagnetic calorimeter and eventually subtract them. However it is clear that measurements of the electromagnetic part of the jet will always be somewhat obscured by the presence of a hadronic background. At LEP energies it will be even the main problem to solve for jet measurement

One way to attack this problem is to simulate jet deposition into calorimeters and see how much of the jet one can reconstruct :

Fig.12a shows the deposition of a simulated 70 GeV jet in the petals of the UA1 Bouchon, assuming no magnetic field (B = 0). Most of the jet energy is concentrated into the two adjacent petals 2 and 3. Since this is a simulation, one can superimpose the points of impact of the individual particles within the jet : there are 5 charged particles (+) and 7 γ's (0), other slow particles belonging to the same jet miss the Bouchon ; 9 particles deposit energy in petals 2 and 3. Turning on the magnetic field to its nominal value, B = 0.7 Tesla, does not help much to separate charged particles from neutrals, as can be seen on fig.12b. Fig.12c shows that at most three energetic clusters can be separated within the jet by using the position detector !

Fig.13a shows another 70 GeV jet in the Bouchon, this time with a large electromagnetic component : a cluster of 6 γ's is going into petal 2, which receives most of the jet energy. Fig.13b shows that there is no hope to separate the 6 γ's, they give only one cluster in the position detector !

It is not necessary to perform further study, to conclude that, in the Bouchon, only the following jet measurements will be available :

(i) Total jet energy, when complementing the bouchon by the end-cap hadronic calorimeter.

(ii) Center of gravity of the jet (first moment). How far is it from the true jet axis ?

(iii) r.m.s. lateral spread of the jet (second moment) To what extent does this spread measure the effective mass of the jet ?

(iv) Electromagnetic energy of the jet. This measurement necessitates a subtraction of the deposited energy by charged particles in the Bouchon. To which precision can one do that ? How much do we gain by having 6 longitudinal readings (4 lead + 2 iron) of the hadronic showers ?

In no way can one hope in UA1 to disentangle individual showers within the jet. Of course one could dream of a much finer lateral segmentation than the one available in UA1. To which extent, this is useful to separate overlapping showers within a jet is an open question for future LEP detectors.

Another relevant question is the use of longitudinal segmentation to measure the electromagnetic component of a jet ; correlations between the first 2 or 3 electromagnetic segments, having a large ratio λ/X_o may help ; this is discussed in a paper written by O.Botner for the ECFA/LEP studies on calorimetry [12].

No doubt that the optimization of a 4π LEP calorimeter will necessitate lots of Monte-Carlo studies. It was the purpose of this talk to indicate to the community that the UA1 approach on shower simulation could be a practical way to solve the problem.

REFERENCES.

1. In the UA1 Collaboration, the construction of all calorimeters is under the responsability of outside institutions, hence mainly physicists from outside laboratories are working on the UA1 calorimeter software. They are :

R.BERNABEI S.d'ANGELO)	University of Roma (INFN)
R.BOCK	CERN
M.J.CORDEN	Birmingham
M.DEBEER	SACLAY
M.DELLA NEGRA	LAPP, Annecy
B.EQUER	Collège de France, Paris
T.P.SHAH	Rutherford, Angleterre

2. "A 4π solid angle detector for the SPS used as a proton-antiproton collider at a centre of mass energy of 540 GeV", CERN/SPSC/78-06, SPSC/P92 (January 1978).

3. More details on the UA1 calorimeter set-up can be found in "Calorimeter Facilities".
A.ASTBURY, Invited talk to this conference.

4. EGS, a Monte-Carlo Program to Simulate Electromagnetic Showers.
R.L.FORD and W.R.NELSON, SLAC-210 (1978).

A Monte-Carlo Calculation of High Energy Hadronic Cascade in Matter.
A.GRANT, NIM 131, 167 (1975).

5. R.BOCK, F.PAGIOLA, J.ZOLL,
Hydra System Manual, CERN.

6. E.LONGO and I.SESTILI,
NIM 128, 283 (1975).

7. M.HOLDER et al., "Performance of a magnetized total absorption calorimeter between 15 GeV and 140 GeV", NIM 151, 317 (1978).

8. M.J.CORDEN et al., "Performance of the UA1 Calorimeter Prototype", Poster Paper submitted to this conference.

9. M.J.CORDEN et al., "Some Hadron Calorimeter Properties Relevant to Storage Rings", Poster Paper Submitted to this conference.

10. B.AUBERT et al., "A Shower Position Detector Inside the Electromagnetic Calorimeter", Presented at the Wire Chamber Conference Vienna 1980, Preprint LAPP 80-03. To be published in Nuclear Instruments and Methods.

11. The Barrel Liquid Argon Counters of TASSO, Preprint in preparation.

12. O.BOTNER, Minimal Calorimeter for Jet Measurements, ECFA/LEP Working Group on Calorimetry.

FIGURE CAPTIONS.

Fig.1. Computer representation of the UA1 Calorimeter set-up : Hydra data structure.

Fig.2. Geometrical tracking : a full event tracked into the UA1 calorimeter system. Straight tracks not extending in the central region are photons not seen by the central detector (track chamber).

Fig.3. Hadronic showers. Parametrization of mean longitudinal profile. The mean pulse height in each scintillator plate is plotted as a function of the depth, expressed in radiation lengths, from the beginning of the shower, for various incident energies. Data are from WA1 [7] on the left (pure iron), from UA1 (pure lead, unpublished data) on the right. The curves are the fits discussed in the text.

Fig.4. Hadronic showers. Parametrization of Mean Longitudinal profile. Data on the left are the same as those on fig.3 left, plotted this time from the beginning of the calorimeter. Data on the right are integrated calorimeter signals as measured by UA1 in a mixed calorimeter consisting of 3 lead segments and 4 iron segments (UA1 - TM 79/50). The curves are predictions from the previous parametrization.

Fig.5. Deposition in scintillator cells.
(a) Integrated of mean deposited energy between s_1 and s_2 using the longitudinal parametrization.
(b) Longitudinal deposition.
(c) Lateral deposition.

Fig.6. Deposition of a 10 GeV π^- beam in the prototype UA1 hadronic calorimeter cell : plot of the visible deposited energy in the back segment versus the visible deposited energy in the front segment.

Fig.7. Same as fig.6 for simulated data.

Fig.8. Deposition of a 10 GeV π^- beam in the prototype UA1 hadronic calorimeter cell :
(a) Distribution of the visible deposited energy in the front segment.
(b) Same in the back segment.
(c) Distribution of the total deposited energy (front + back).
The curves result from the simulation discussed in the text.

Fig.9. Reconstruction of a single electromagnetic shower in a half-Bouchon (UA1 end cap electromagnetic calorimeter) exposed to 40 Gev e^- beam :
(a) Horizontal tubes.
(b) Vertical tubes.
(c) Petals superimposed to position detector information.

Fig.10. A single electromagnetic shower from a Bhabba event at $\sqrt{S}$ = 35.5 GeV in the Liquid Argon TASSO calorimeter.
(a) Side view of calorimeter.
(b) Front view of calorimeter showing the deposition in the front towers and the back towers. Also shown are the signals in the Z-strips and the ϕ-strips.

Fig.11. A hadronic jet, E_{jet} = 17.5 GeV, in the Liquid Argon TASSO calorimeter
(a) Side view.
(b) Front view.

Fig.12. A simulated 70 GeV jet into the Bouchon : hits of charged particles are represented as : +, hits of photons are represented as : O
(a) No magnetic field : B = 0.
(b) With magnetic field : B = 0.7 Tesla.
(c) Position detector information (vertical tubes only)

Fig.13. A simulated 70 GeV jet, having a large electromagnetic component, into the Bouchon
(a) Petals and hits.
(b) Position detector information (vertical tubes only).

COMPUTER REPRESENTATION OF DETECTOR

HYDRA DATA STRUCTURE

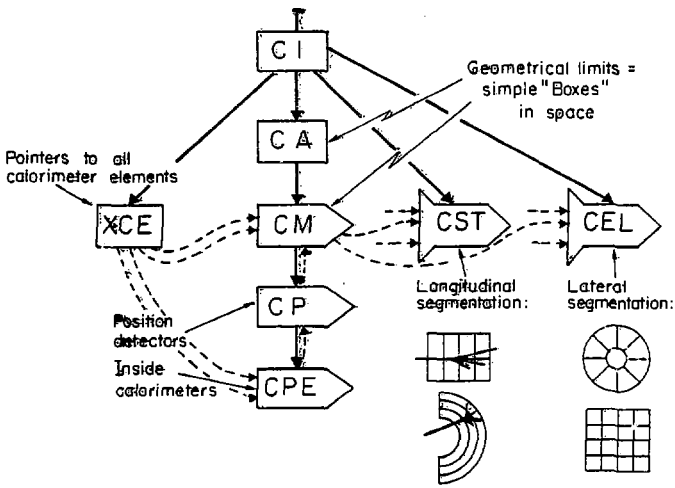

Fig. 1

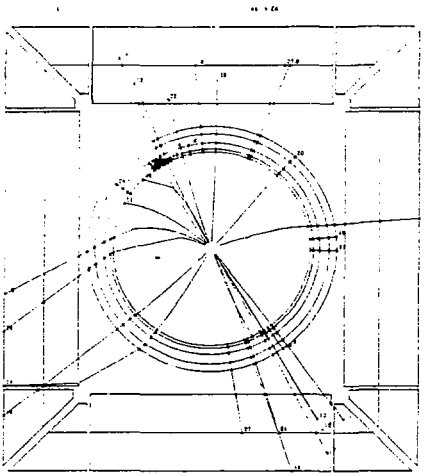

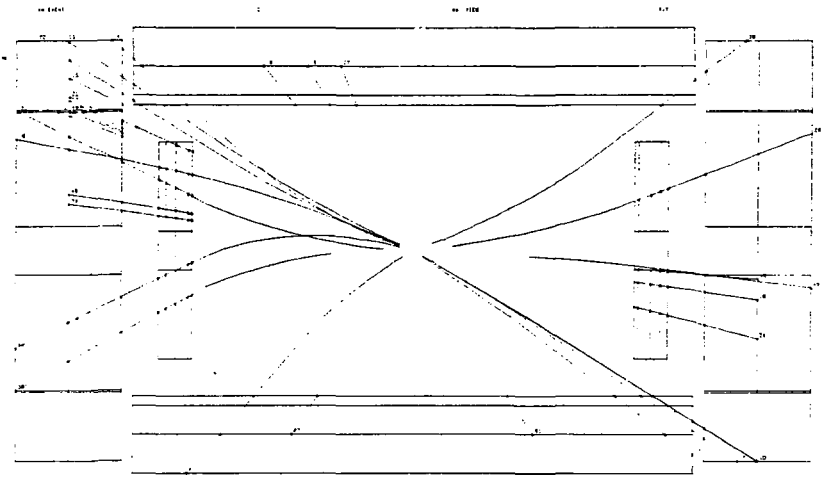

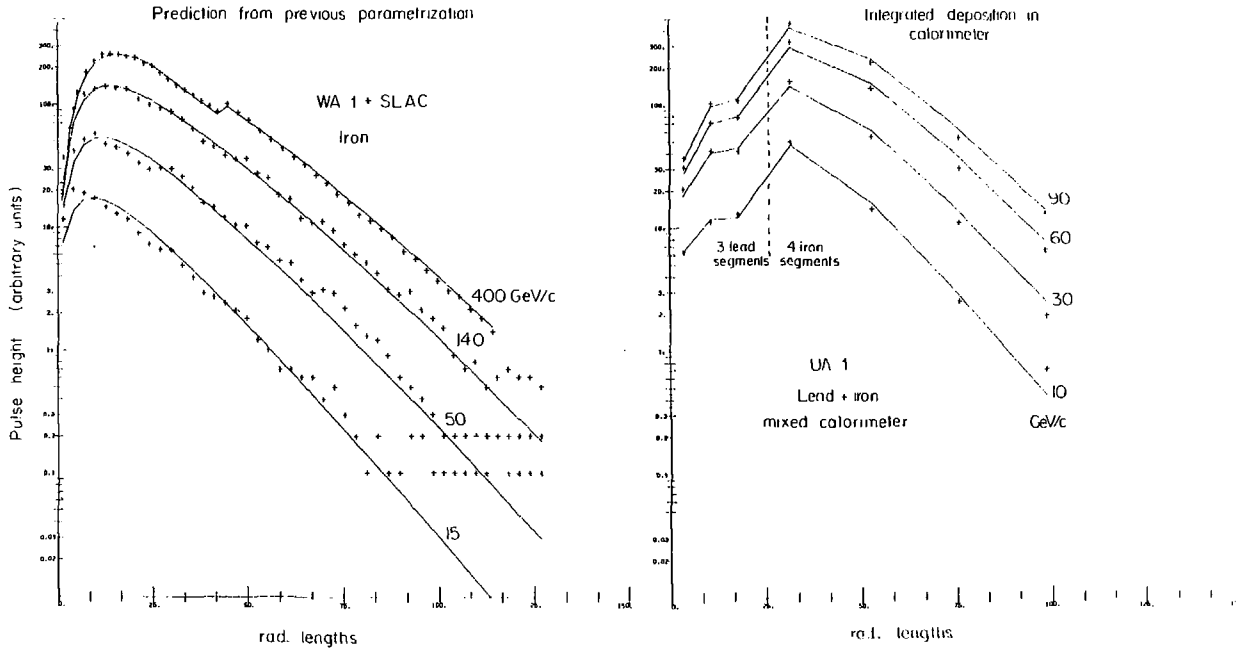
Prediction from previous parametrization
WA 1 + SLAC
Iron
400 GeV/c
140
50
15
Pulse height (arbitrary units)
rad. lengths
Integrated deposition in calorimeter
3 lead segments
4 iron segments
90
60
30
10
UA 1
Lead + iron
mixed calorimeter
GeV/c
rad. lengths

Fig. 3

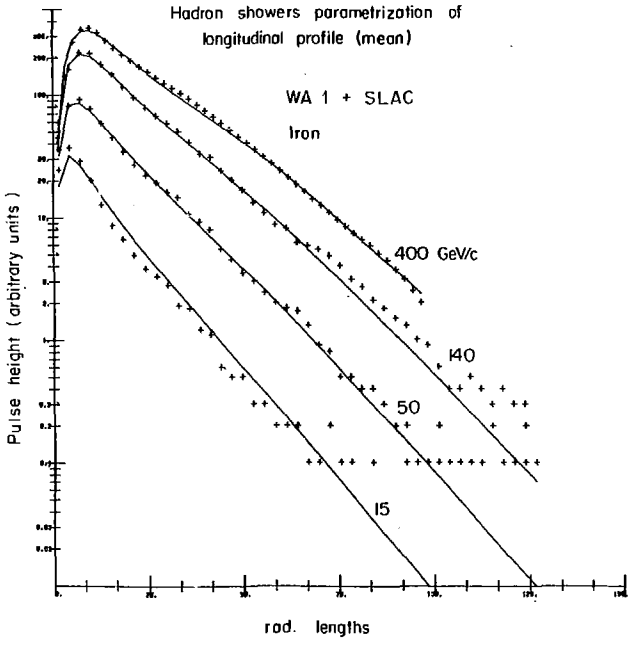
Hadron showers parametrization of
longitudinal profile (mean)
WA 1 + SLAC
Iron
400 GeV/c
140
50
15
Pulse height (arbitrary units)
rad. lengths

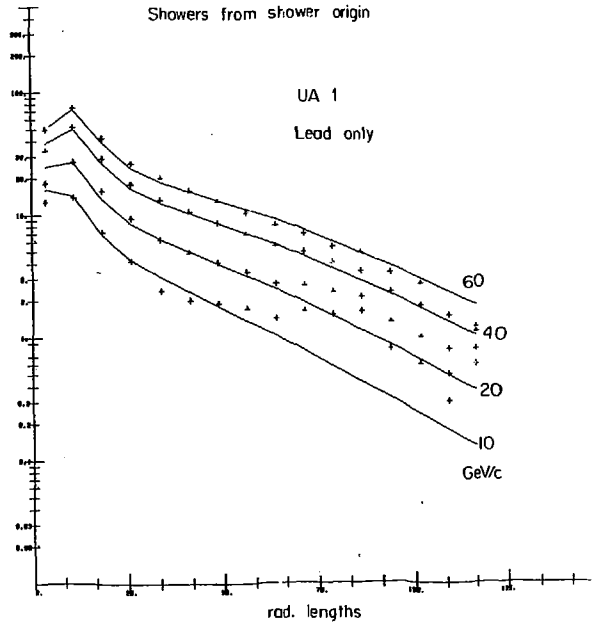
Showers from shower origin
UA 1
Lead only
60
40
20
10
GeV/c
rad. lengths

Fig. 4

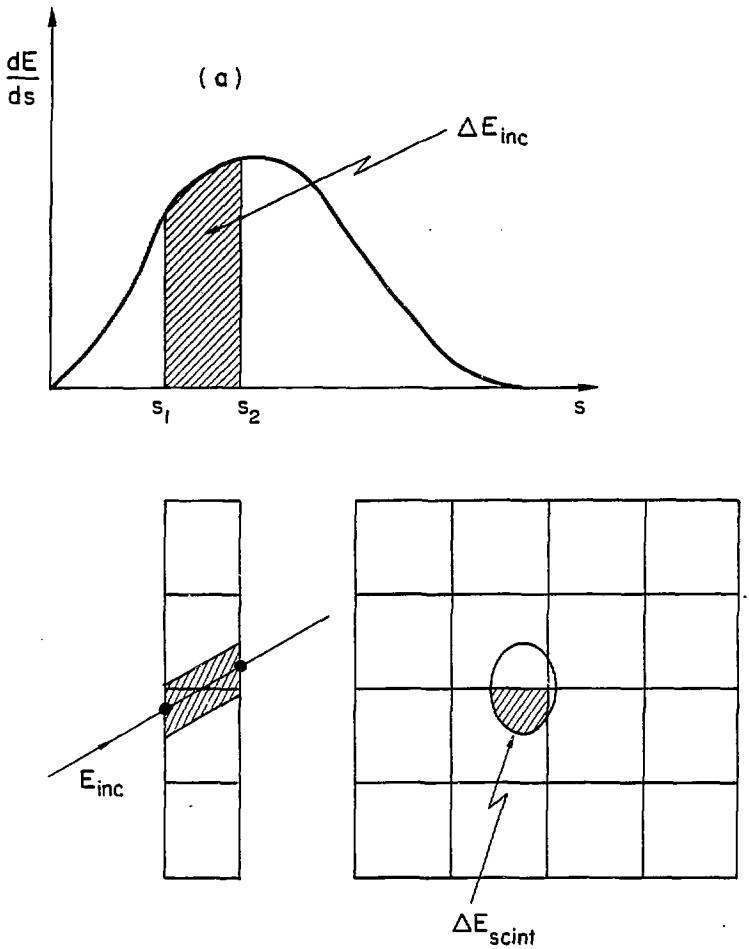

Fig.5

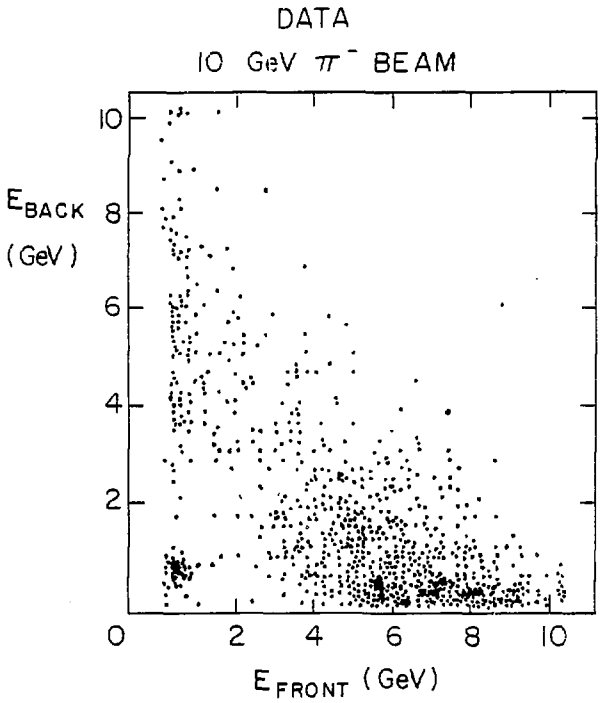

Fig.6

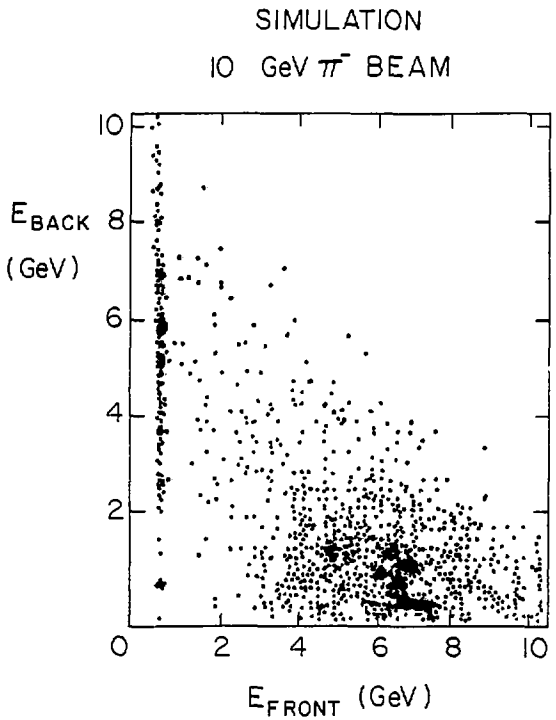

Fig. 7

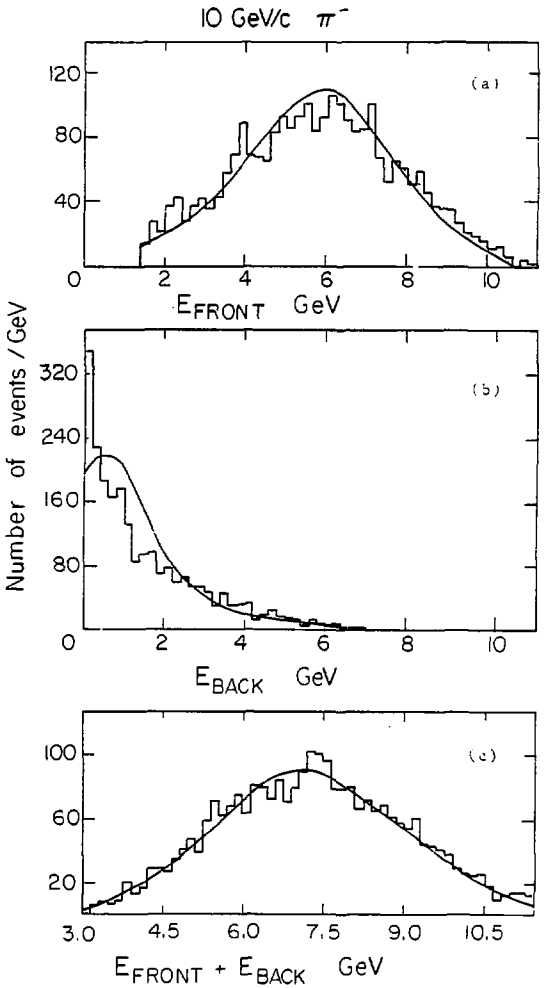
10 GeV/c π⁻
(a)
120
80
40
0
2
4
6
8
10
E FRONT GeV
Number of events / GeV
(b)
320
240
160
80
0
2
4
6
8
10
E BACK GeV
(c)
100
60
20
3.0
4.5
6.0
7.5
9.0
10.5
E FRONT + E BACK GeV

Fig. 8

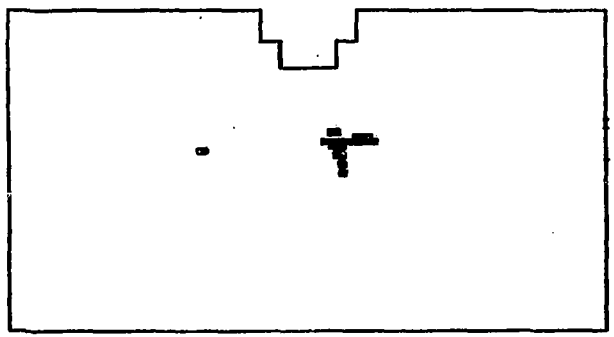

Fig.9a)

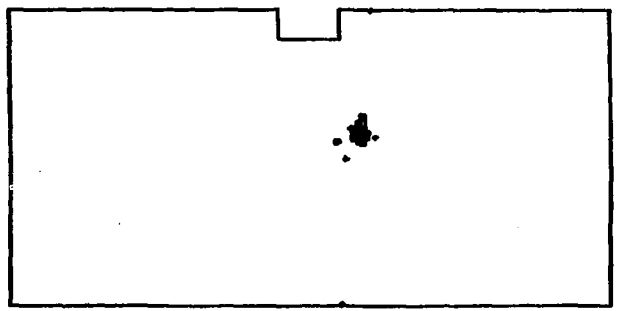

Fig.9b)

-10 0 0 4 1 -11 42 400 806 13 -12 0 0 0 0

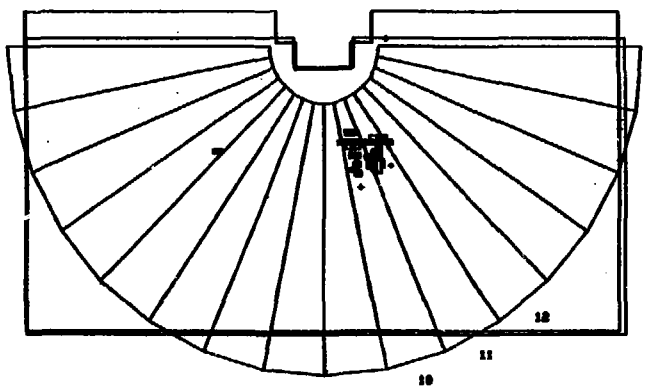

Fig.9c)

FIFHEY.APABHAI RUN 2128 EVENT 559 EBEAM= 17.61 GEV TRIGGER= 0100100100000001 VERSION 6.7
DATE 29/05/80

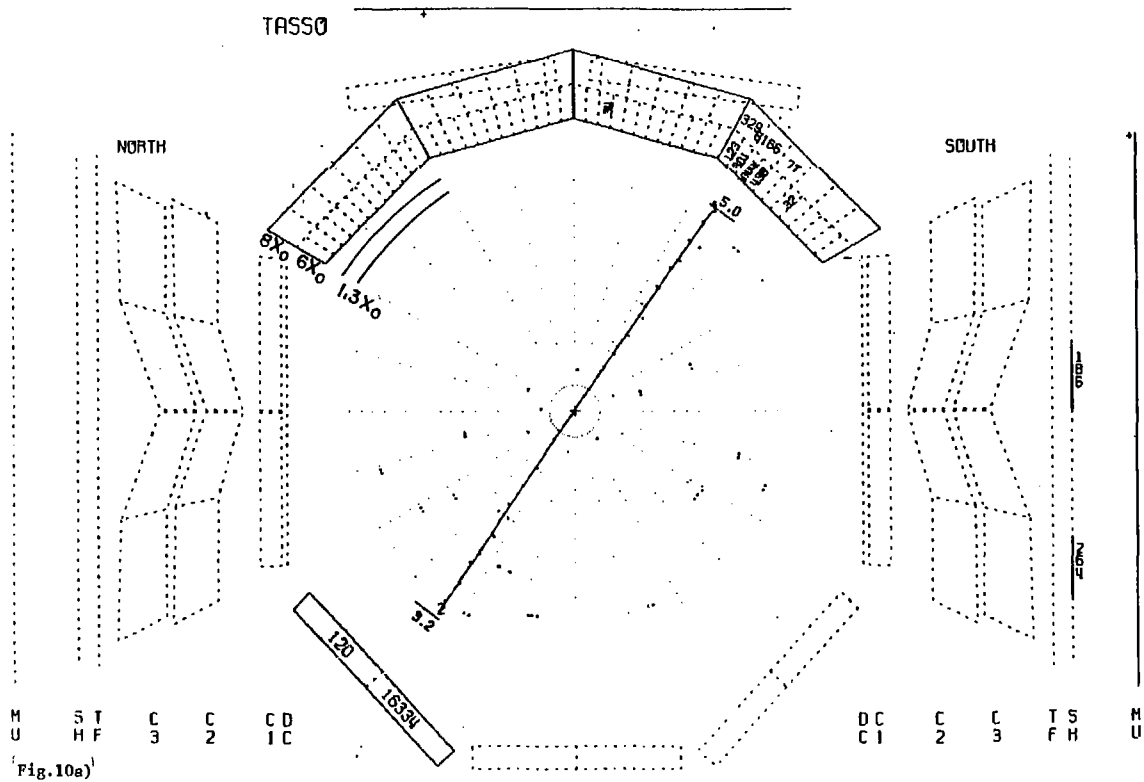

Fig.10a)

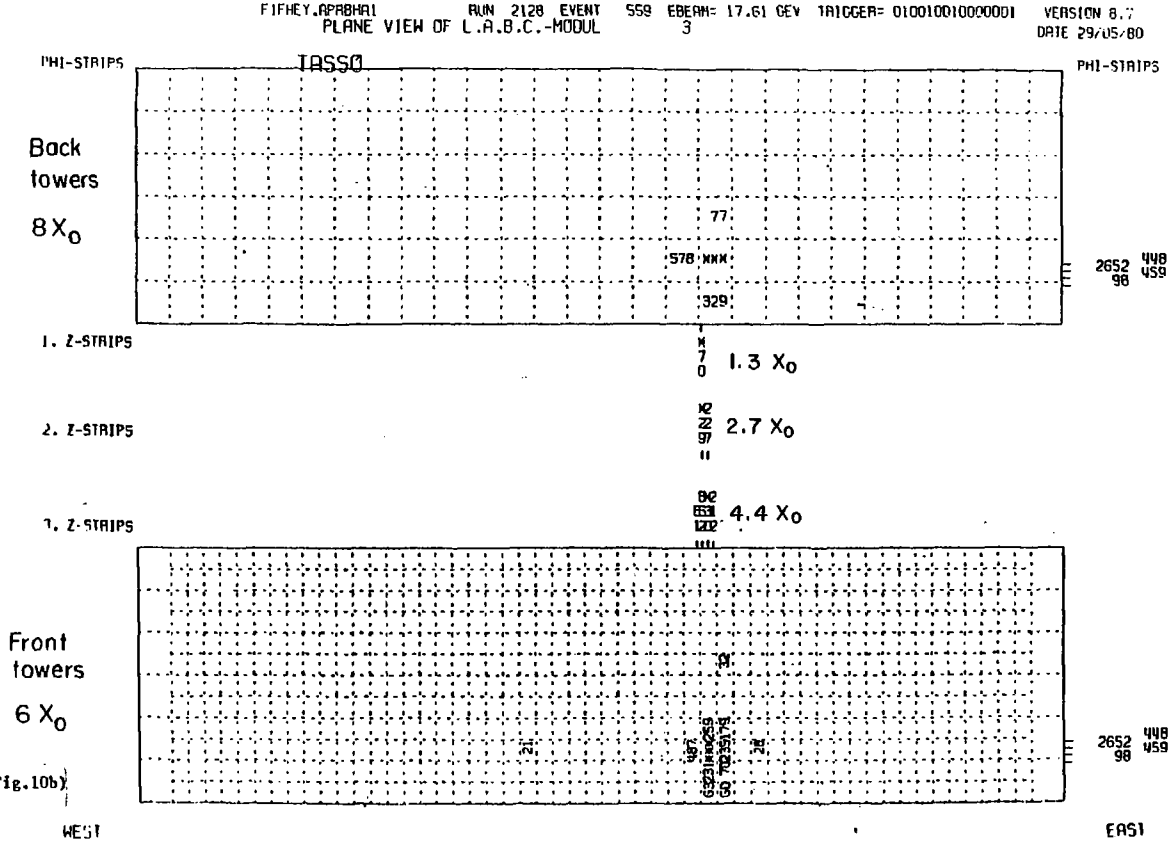
FIFHEY.APABHAI RUN 2128 EVENT 559 EBEAM= 17.61 GEV TRIGGER= 0100100100000001 VERSION 8.7
PLANE VIEW OF L.A.B.C.-MODUL 3 DATE 29/05/80
TASSO
PHI-STRIPS
PHI-STRIPS
Back towers
8 X0
77
578
329
2652 448
98 459
1. Z-STRIPS
1.3 X0
2. Z-STRIPS
2.7 X0
3. Z-STRIPS
4.4 X0
Front towers
6 X0
2652 448
98 459
WEST
EAST

Fig.10b)

TASS02.HADSCAN.TEMPH RUN 2284 EVENT 5785 EBEAM= 17.75 GEV TRIGGER= 0100100100000001 VERSION 8.7
DATE 29/05/80

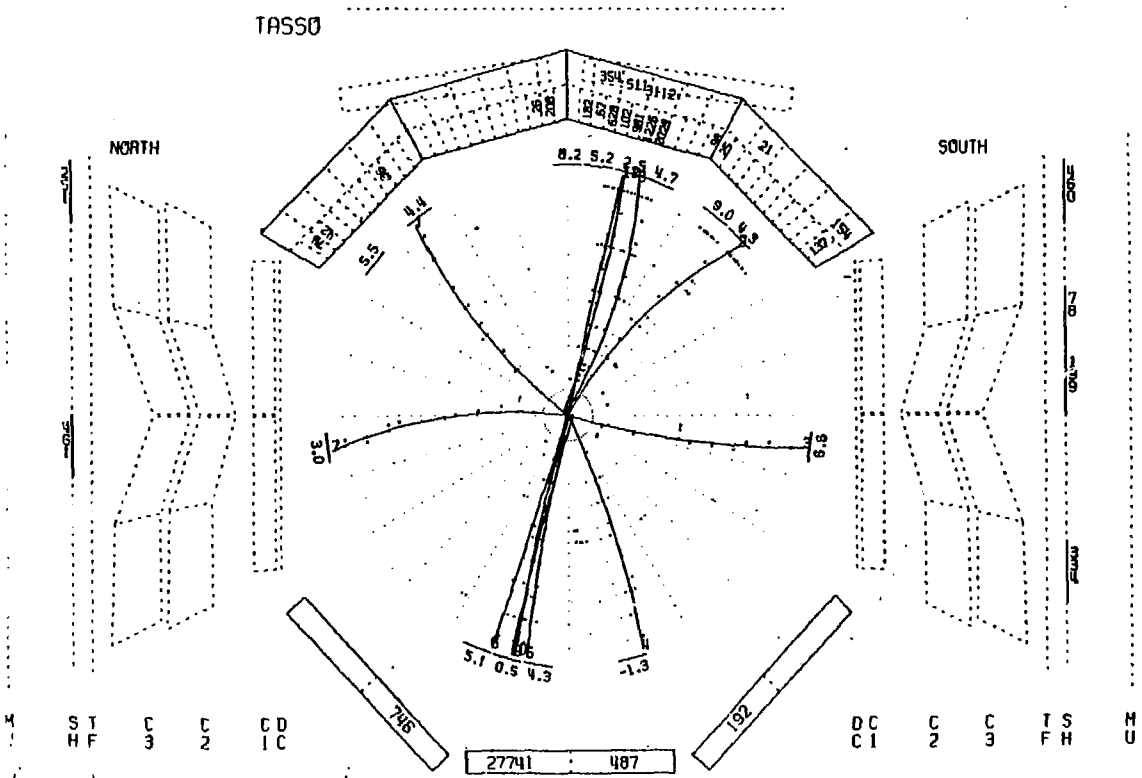

Fig.11a)

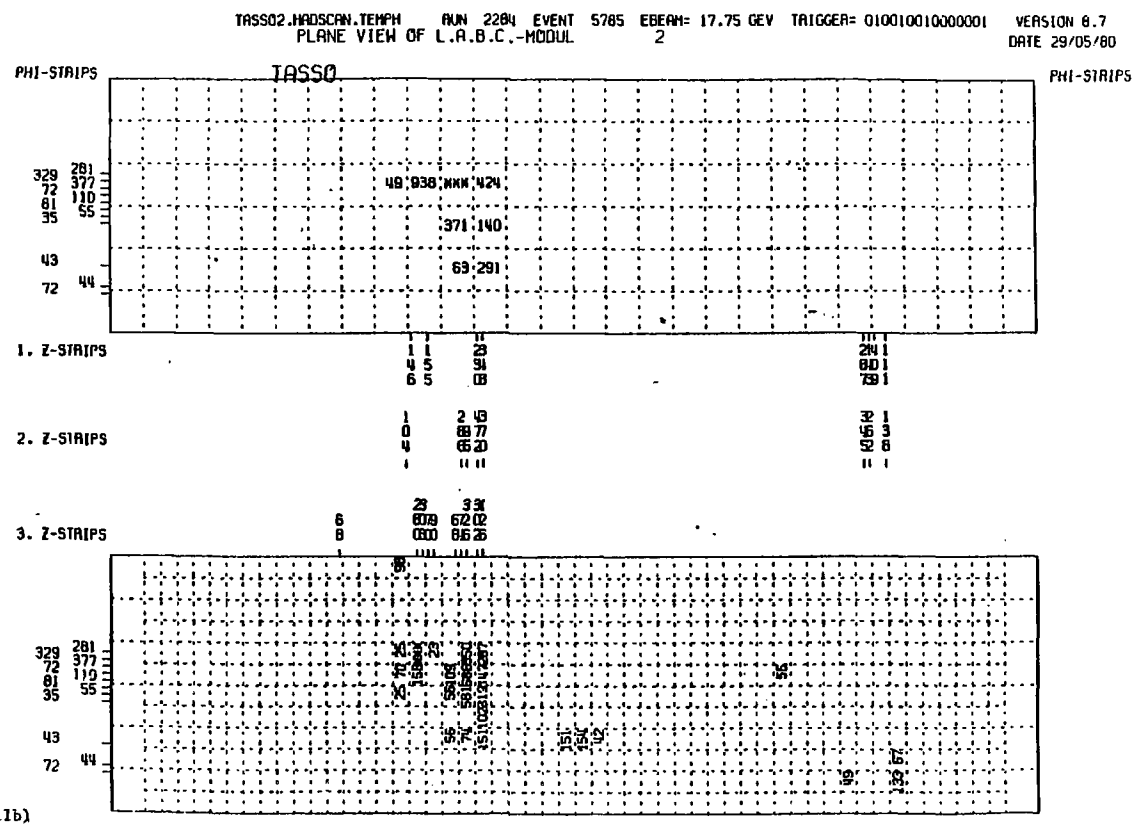
TASS02.HADSCAN.TEMPH RUN 2284 EVENT 5785 EBEAM= 17.75 GEV TRIGGER= 0100100100000001 VERSION 8.7
PLANE VIEW OF L.A.B.C.-MODUL 2
DATE 29/05/80
TASSØ
PHI-STRIPS
PHI-STRIPS
1. Z-STRIPS
2. Z-STRIPS
3. Z-STRIPS
WEST
EAST

Fig.11b)

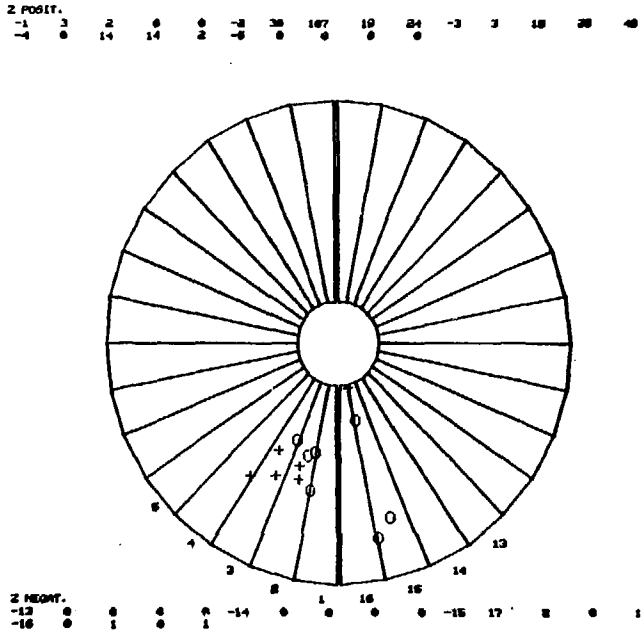

Fig.12a)

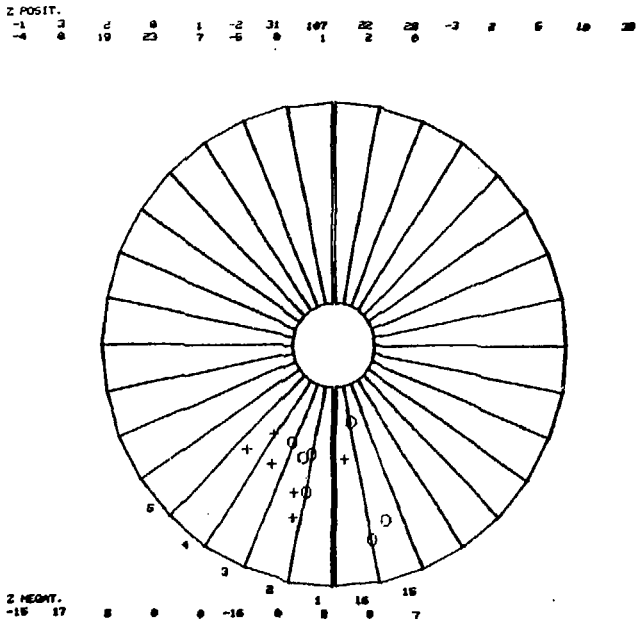
Z POSIT.
-1 3 -6 0 1 -2 31 107 22 28 -3 2 5 19 28
-4 0 19 23 7 -5 0 1 2 0
5
4
3
2
1
16
15
Z HEGHT.
-15 17 5 0 0 -16 0 8 0 7

Fig.12b)

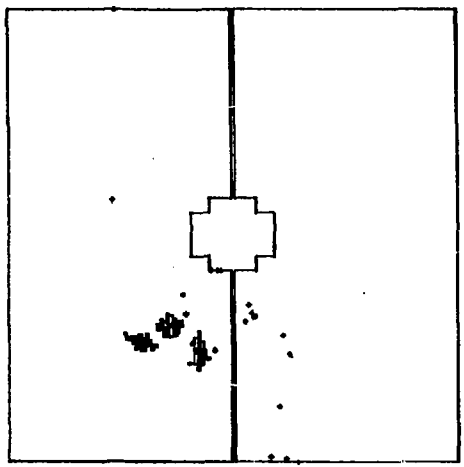

Fig.12c)

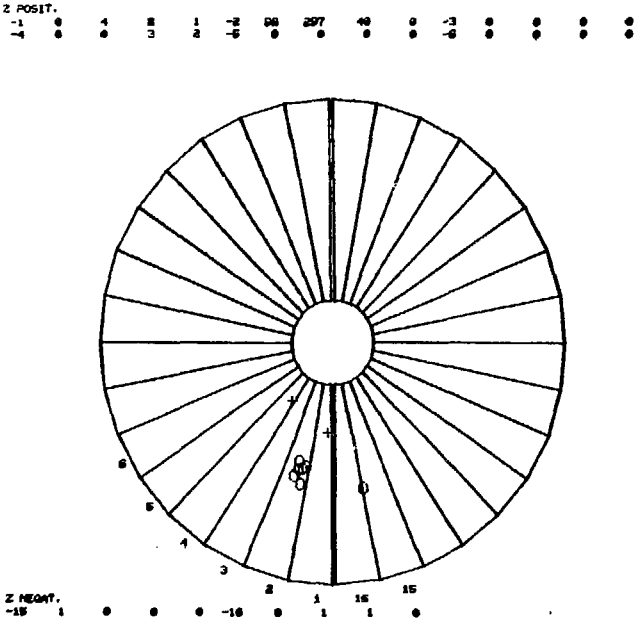

Fig.13a)

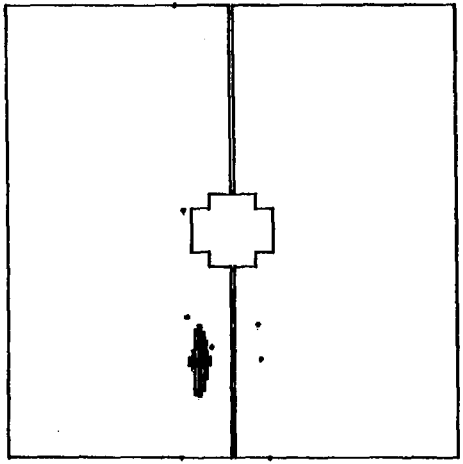

Fig.13b)